Nuclear Engineering and Technology 53 (2021) 4122–4129

Contents lists available at ScienceDirect

Nuclear Engineering and Technology

journal homepage: www.elsevier.com/locate/net

Original Article

Virtual calibration of whole-body counters to consider the size dependency of counting efficiency using Monte Carlo simulations

MinSeok Park [a, b, *], Han Sung Kim [a, b], Jaeryong Yoo [a], Chan Hyeong Kim [b], Won Il Jang [a], Sunhoo Park [a]

[a] National Radiation Emergency Center, Korea Institute of Radiological and Medical Sciences, Seoul, 01812, Republic of Korea
[b] Department of Nuclear Engineering, Hanyang University, Seoul, 04763, Republic of Korea

ARTICLE INFO

Article history:
Received 25 February 2021
Received in revised form
31 May 2021
Accepted 12 June 2021
Available online 17 June 2021

Keywords:
Counting efficiency
Whole-body counter
Monte Carlo simulation
Computational phantom

ABSTRACT

The counting efficiencies obtained using anthropomorphic physical phantoms are generally used in whole-body counting measurements to determine the level of internal contamination in the body. Geometrical discrepancies between phantoms and measured individuals affect the counting efficiency, and thus, considering individual physical characteristics is crucial to improve the accuracy of activity estimates. In the present study, the counting efficiencies of whole-body counting measurements were calculated considering individual physical characteristics by employing Monte Carlo simulation for calibration. The NaI(Tl)-based stand-up and HPGe-based bed type commercial whole-body counters were used for calculating the counting efficiencies. The counting efficiencies were obtained from 19 computational phantoms representing various shapes and sizes of the measured individuals. The discrepancies in the counting efficiencies obtained using the computational and physical phantoms range from 2% to 33%, and the results indicate that the counting efficiency depends on the size of the measured individual. Taking into account the body size, the equations for estimating the counting efficiencies were derived from the relationship between the counting efficiencies and the body-build index of the subject. These equations can aid in minimizing the size dependency of the counting efficiency and provide more accurate measurements of internal contamination in whole-body counting measurements.

1. Introduction

Radiological release into the environment due to nuclear accidents cause internal contamination in workers and the general public, and measuring the internal contamination in potentially exposed individuals is crucial in mitigating possible health risks. *In vivo* measurement of radioactive materials retained in the human body is a primary method for estimating the internal contamination from X-ray or gamma ray-emitting radionuclides [1]. In response to the Fukushima nuclear accident, population monitoring, which includes whole-body counting measurements, was performed to assess the internal exposure of the residents of the Fukushima prefecture [2–4].

Whole-body counters (WBCs) are conventionally employed in *in vivo* measurements of internal contamination. Calibrating WBCs is essential to ensure the accuracy of activity estimates in *in vivo* measurements. WBC calibration may be performed using the bottle manikin absorber (BOMAB) phantom [5], which is a simple physical phantom composed of ten cylindrical polyethylene bottles filled with a radioactive solution of known activity to estimate the calibration factor.

Despite the simplicity of operation, there are several problems associated with the use of BOMAB phantom in WBC calibration. The similarity in anatomical characteristics between the physical phantom and the measured human is an important parameter that can influence the measurement accuracy, especially the counting efficiency [6–10]. The BOMAB phantom, however, does not reflect different body types accurately since the phantoms comprise polyethylene bottles and do not include the bones and internal organs. The geometrical discrepancies between the BOMAB phantom and measured individuals influences the results of whole-body measurements, due to the over- or under-estimation of counting efficiency [11]. To address this issue, it is necessary to consider individual physical characteristics in whole-body counting

* Corresponding author. National Radiation Emergency Center, Korea Institute of Radiological and Medical Sciences, Seoul, 01812, Republic of Korea.
E-mail address: chulipak@kirams.re.kr (M. Park).

https://doi.org/10.1016/j.net.2021.06.026

measurements. Another issue is related to the management of radioactive substances. Leakage is a potential issue in the use of BOMAB phantom, as aqueous radioactive solutions are used in it. This leakage can contaminate the counting system, where a low background environment is desired in *in vivo* measurements [12]. In addition, BOMAB phantom generates liquid radioactive waste, and managing this waste is a concerning issue [13]. Finally, BOMAB phantom is not cost-effective. Thus, it is impractical to construct BOMAB phantoms for different body sizes [14].

To overcome these limitations, Monte Carlo methods have been used previously to calibrate *in vivo* measurement systems. Monte Carlo simulations estimate the counting efficiency of WBCs using virtual representations of counting systems and source objects [10]. Recent advances in computational phantoms has led to the simulation of realistic human models with Monte Carlo methods [8,15]. Computational phantoms can be constructed from computed tomography, magnetic resonance imaging, or anatomical photographs of cadavers, which represent detailed anatomical information of real human bodies. Using computational phantoms to calibrate *in vivo* measurement systems can improve the accuracy of the measurements [15–18]. Therefore, this study aims to estimate the counting efficiency by taking into account the physical characteristics of individuals in whole-body counting measurements. This study describes the virtual calibration of WBCs, which was achieved by Monte Carlo simulations with the computational phantoms of different sizes developed by different research groups to derive the equations for estimating the individualized counting efficiencies in the whole-body measurement.

2. Materials and methods

Two commercial WBCs at the Korea Institute of Radiological and Medical Sciences (KIRAMS) were used in this study: a stand-up type WBC system (FASTSCAN; Canberra Industries, Meriden, CT, USA) with upper and lower NaI(Tl) detectors having the crystal dimensions of 7.6 cm × 12.7 cm × 40.6 cm and a bed type WBC system (ACCUSCAN; Canberra Industries, Meriden, CT, USA) with two high-purity germanium (HPGe) detectors having the crystal dimensions of 6.2 cm (diameter) × 4.1 cm (length) and 6.2 cm (diameter) × 3.6 cm (length). The detectors in the WBCs were shielded by 10 cm of low background steel to minimize the influence of the background radiation. Based on the manufacturer specifications, WBCs were simulated using a Monte Carlo code for *in vivo* measurements. The geometries of the stand-up and bed type WBCs are shown in Fig. 1. Unlike the stand-up type WBC with static measurement geometry, the scanning bed automatically moves the individuals through the detection system in the bed type WBC. The movement of the scanning bed in the bed type WBC makes simulation difficult, because most Monte Carlo codes employ static geometries [19]. Therefore, we modified the simulation geometry of the bed type WBC, representing a complete continuous scan as a sum of discretized steps [13,20]. As shown in Fig. 1b, the detection systems of the bed type WBC were arranged in 12 horizontal positions to optimize the computational time and the scanning movement. Based on this modified geometry, the counting efficiencies for the bed type WBC were calculated in a single simulation.

The simulation geometries of the WBCs have been validated previously [13], and the relative deviations of the counting efficiencies between the measurements and the simulation for the BOMAB phantom were less than 9% (averaged relative deviations were 4.8% and 4.6% in the stand-up and bed type WBCs, respectively). The Monte Carlo simulation was performed with the Monte Carlo N-Particle transport code (MCNP6.2) developed by the Los Alamos National Laboratory [21].

The counting efficiencies for each photopeak in the pulse height spectrum were obtained using the F8 tally (pulse-height tally) of the MCNP code. The energy bins of the pulse height spectra from the stand-up and bed type WBCs are composed of 512 and 8192 channels, respectively. The Gaussian energy broadening function was applied to the F8 tally to simulate the energy resolution of the detection system. This is based on the full-width at half-maximum from the calibration curve of the detectors of the WBCs. The number of source particles used in each simulation was 5×10^8 to maintain the statistical uncertainties of the tally results below 5%. The reliability of the tally results can be checked based on the statistical uncertainties. Statistical uncertainties of <10% indicate that the results are reliable [21].

We used 19 computational phantoms developed by several research groups to represent the anatomical characteristics of measured individuals. These include the International Commission on Radiological Protection (ICRP) adult reference computational phantoms [22], the University of Florida/National Cancer Institute (UF/NCI) reference hybrid family phantoms [23], high definition reference Korean (HDRK) phantoms [24,25], visible photographic man (VIP-Man) phantom [26], Japanese adult (JM, JF) voxel phantoms [27,28], and male/female adult mesh (MASH, FASH) phantoms [29]. The anatomical information of adult males and females was represented in all of the computational phantoms except for the VIP-Man phantom, which included information of only adult males. The UF/NCI reference hybrid family phantom also involved the anatomical information of pediatric males and females aged 1 y, 5 y, 10 y, and 15 y. Various computational phantoms including the pediatric case were used in the present study to investigate the influence of physical characteristics on the counting efficiency in the whole-body counting measurement. An overview of the computational phantoms used in the present study is presented in Table 1. Each computational phantom represents different physical characteristics, including height and weight. The basic data (or images) and construction methods for the computational phantoms varied for different phantoms. The body-build index (BBI) of each computational phantom was calculated from the corresponding weight and height data. The BBI is defined as $(W/H)^{1/2}$, where W and H are the weight (kg) and height (cm) of the measured individual, respectively. The BBI was used to estimate the subject size [30].

The stand-up and bed type WBCs modeled with the Monte Carlo code as represented in Fig. 1 were applied to the computational phantoms to calculate the counting efficiencies. The calibration of the WBCs was conventionally performed using the BOMAB phantom with homogeneously distributed radioactivity within the bottles. Moreover, the calibration of the WBCs was performed based on the assumption that the measured individual was homogeneously contaminated. Thus, the radioactive source in the computational phantom simulated the homogeneous distribution throughout all tissues except the skin [8].

The computational phantoms, except for the 1 y, 5 y, and 10 y-old pediatric computational phantoms, were located in the WBCs at positions equivalent to those of the BOMAB adult phantom to reproduce the calibration conditions. This approach, however, would result in a significant underestimation of the counting efficiencies for the 1 y, 5 y, and 10 y-old pediatric computational phantoms due to the fact that the lower side detector of the stand-up type WBC was placed 61 cm above its bottom so as to mainly view the adult torso [2]. Note that in practice of pediatric measurement, a stool or lift was used to increase the sensitivity of the stand-up type WBC. In the present study, therefore, the positions of the 1 y, 5 y, and 10 y-old pediatric computational phantoms were elevated considering the practice of pediatric measurements. As represented in Table 2, the positions for the 1 y, 5 y, and 10 y-old pediatric computational phantoms in the stand-up type WBC were

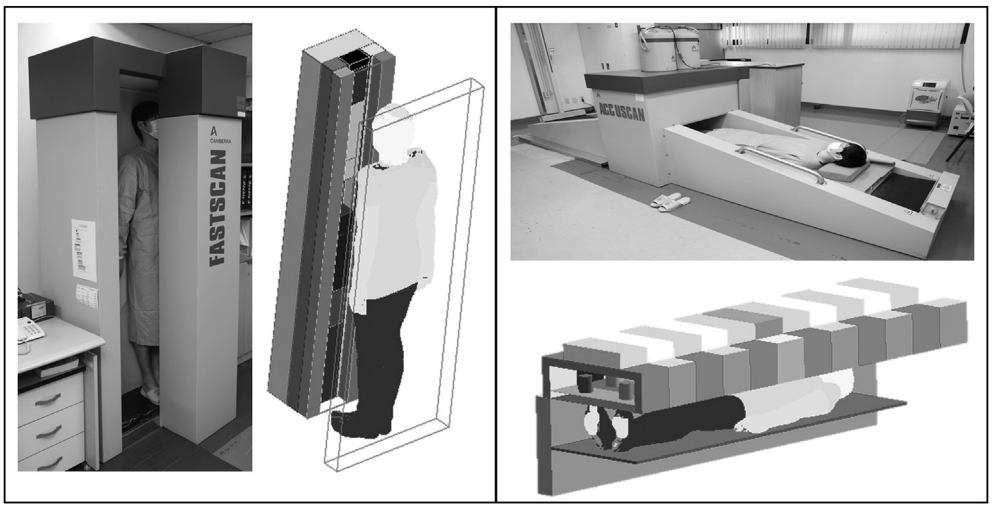

Fig. 1. Photographs and computational modeling geometry of the WBCs: (a) stand-up type WBC, (b) bed type WBC.

Table 1
Anatomical characteristics of the male and female computational phantoms.

Phantom	Gender	Height (cm)	Weight (kg)	Body build index $(W/H)^{1/2}$
ICRP	male	176	73	0.66
	female	163	60	0.61
HDRK	male	172	68	0.63
	female	761	54	0.58
VIP-Man	male	186	103	0.74
JM, JF	male	171	65	0.62
	female	152	44	0.54
MASH, FASH	male	175.6	73	0.64
	female	162.5	60	0.61
UF/NCI Adult	male	176	73.4	0.65
	female	163	59.7	0.61
UF/NCI 1 y	male	76	10	0.36
	female	76	10	0.36
UF/NCI 5 y	male	109	18	0.41
	female	109	18	0.41
UF/NCI 10 y	male	138	32	0.48
	female	138	32	0.48
UF/NCI 15 y	male	167	57	0.58
	female	161	53	0.56

determined based on the height of the ICRP adult reference computational phantoms.

Counting efficiencies were determined for the gamma ray energies of 59.5, 88.0, 122.1, 165.9, 391.7, 661.6, 898.0, 1173.2, 1332.5, and 1836.1 keV, emitted from the radionuclides ^{241}Am, ^{109}Cd, ^{57}Co, ^{139}Ce, ^{113}Sn, ^{137}Cs, ^{60}Co, and ^{88}Y, respectively. The calculated counting efficiencies for the BOMAB and computational phantoms were compared to investigate the influence of geometrical discrepancies between the physical calibration phantoms and computational phantoms on the counting efficiencies for both WBCs.

The measured individuals have a heterogeneous tissue distribution; however, the BOMAB phantom describes a simplified human anatomy with homogeneous tissue distribution. Thus, it is necessary to evaluate the effect of tissue homogeneity (in terms of the densities and composition of the internal organs) on the whole-body counting measurement. The densities and material compositions of all internal organs in the computational phantoms were changed to those of water except for the skin. Monte Carlo simulations were performed with the modified (i.e., water-filled) computational phantoms to investigate the influence of tissue distribution of the internal organs on the whole-body measurement. The counting efficiencies obtained from the computational phantoms were compared with those obtained from the modified computational phantoms.

The counting efficiencies are influenced by the anatomical characteristics of the individual, especially the body size. The effect of the body size on the counting efficiency should be corrected to improve the accuracy of whole-body measurements. Significant correlations between the counting efficiency and subject size in whole-body counting measurements have been reported previously [30,31]. In the present study, the relationship between the counting efficiency and subject size was investigated to derive an equation for estimating the individualized counting efficiencies for both WBCs. The subject size can be estimated using the BBIs presented in Table 1. This parameter indicates the average body thickness of the individuals [31]. To establish the relationship between the counting efficiencies and subject size, the counting efficiencies for the 19 computational phantoms were evaluated at the gamma ray energies 122.1, 604.7, 661.6, and 1173.2 keV, emitted from ^{57}Co, ^{134}Cs, ^{137}Cs, and ^{60}Co, respectively. These radionuclides are the main contributors to internal contamination in nuclear accidents.

Table 2
Modified positions of the pediatric computational phantoms in the stand-up type WBC.

Phantom	1 y		5 y		10 y	
Gender	male	female	male	female	male	female
Modified positions from the bottom of stand-up type WBC (cm)[a]	34.6	33.2	22.9	20.9	12.7	10.1

[a] The modified positions were calculated based on the ratios of the height for the ICRP adult reference computational phantom relative to the position of the lower detector (61 cm) on the stand-up type WBC (Male: 34%, Female: 36%).

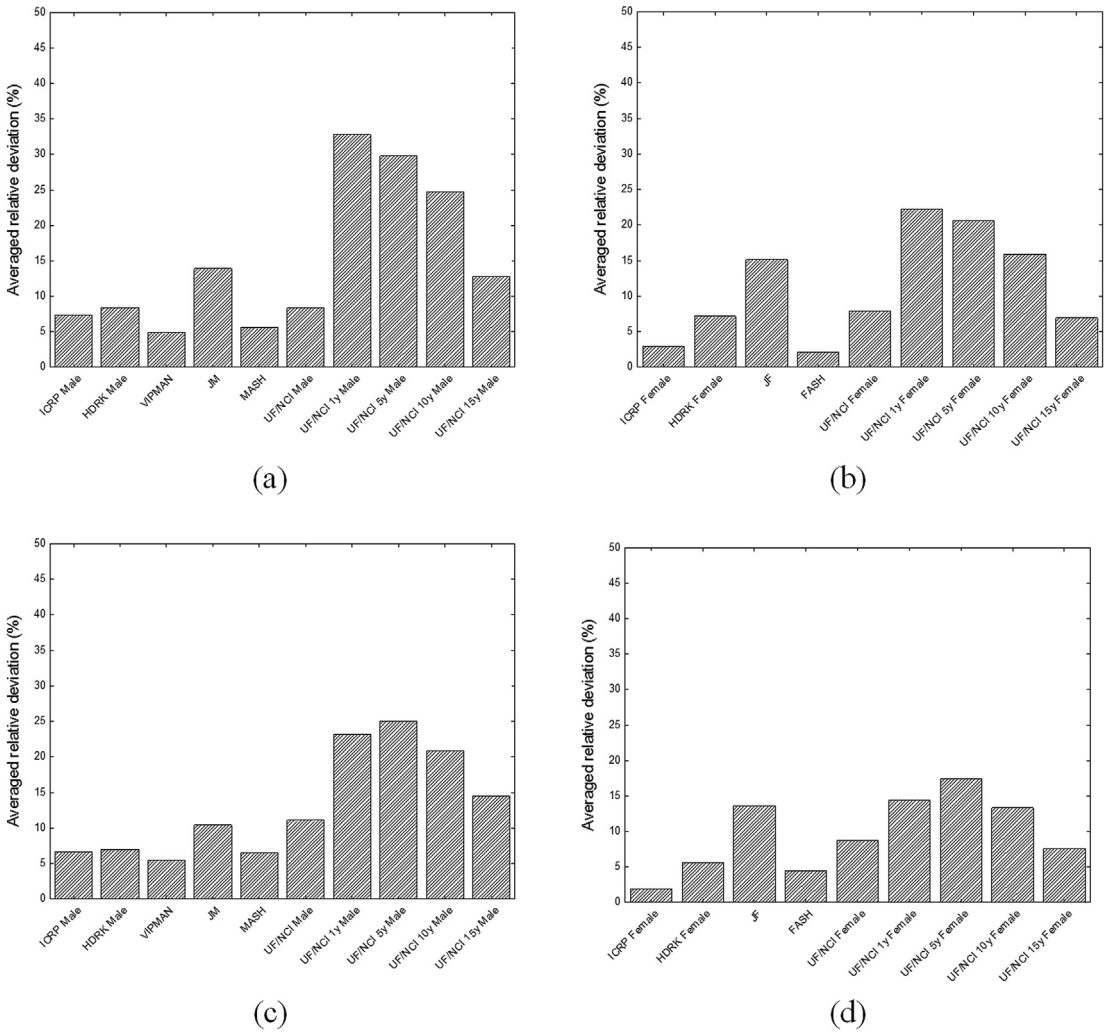

Fig. 2. Averaged deviations of counting efficiencies calculated using computational phantoms from those obtained with BOMAB adult phantom: (a) male phantoms in the stand-up type WBC, (b) female phantoms in the stand-up type WBC, (c) male phantoms in the bed type WBC, and (d) female phantoms in the bed type WBC.

3. Results and discussion

The counting efficiencies calculated using the computational phantoms were compared with those calculated using the BOMAB adult phantom for each gender. The counting efficiencies obtained from the pediatric computational phantoms were also included in this comparison to investigate the dependence of counting efficiencies on the body size. The averaged relative deviations between the counting efficiencies of the BOMAB and computational phantoms for the stand-up and bed type WBCs are shown in Fig. 2. The deviations are within the range of 2%–33%, considering all phantoms and both whole-body measurement systems. The counting efficiencies of the VIP-Man, ICRP, female, and FASH computational phantoms are in good agreement (<5% deviation) with those of the BOMAB adult phantom. Meanwhile, relatively large discrepancies are observed in the pediatric computational phantom of the UF/NCI as well as JM and JF computational phantoms for both WBCs. The counting efficiencies for these computational phantom groups are over 10% greater than those for the BOMAB adult phantom. In particular, the differences in the counting efficiencies between the BOMAB adult phantom and the 1 y-old male UF/NCI computational phantoms are 33% and 23% for the stand-up and bed type WBCs, respectively. These differences in the counting efficiencies are owing to the body size of the computational phantoms in the measurement geometry of the WBCs. These computational phantoms have smaller heights and lower weights compared to the BOMAB and other computational phantoms.

Additional simulations were performed to investigate the discrepancies in the counting efficiencies between the calibration phantoms and the measured individuals for the pediatric cases. As shown in Fig. 3, the calculated efficiencies of the 5 y and 10 y-old UF/NCI pediatric computational phantoms were compared to those of the 4 y and 10 y-old BOMAB phantoms, respectively. The counting efficiencies of the pediatric computational phantoms for both of WBCs are over 7% larger than those of BOMAB phantoms.

The comparison results demonstrate that the geometrical differences between the measured individual and the physical calibration phantom influence the counting efficiency. A similar trend in deviations is observed in the stand-up and bed type WBCs. However, the discrepancies for the bed type WBC are smaller than those for the stand-up type WBC. This result indicates that individual's physical characteristics have less influence on the counting efficiency in the bed type WBC than in the stand-up type WBC, owing to the difference between the counting geometry for

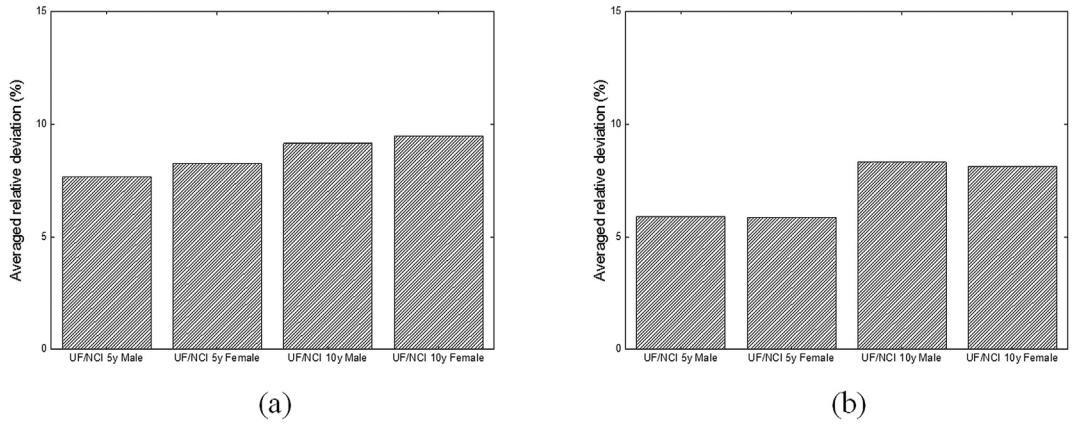

Fig. 3. Averaged deviations of counting efficiencies calculated with pediatric (5 y and 10 y) computational phantoms from those obtained with 4 y and 10 y old BOMAB phantoms for (a) stand-up type WBC and (b) bed type WBC.

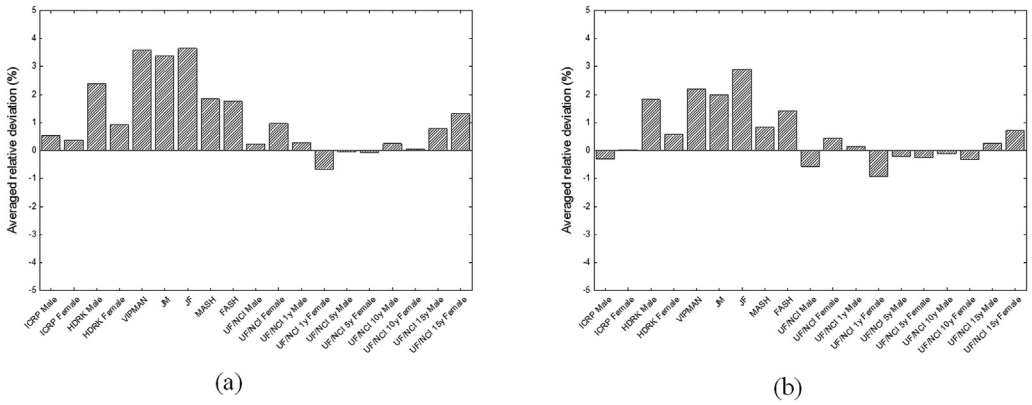

Fig. 4. Comparison of counting efficiencies between the original computational phantoms and modified homogeneous computational phantoms for both whole-body measurement systems: (a) stand-up type WBC, (b) bed type WBC.

both systems. Note that the counting geometry of the bed type WBC covers the entire body of the individual under inspection due to the movement of the scanning bed when performing measurements, while the stand-up type WBC uses two large NaI(Tl) detectors positioned toward the torso of the individual in a static measurement geometry.

Fig. 4 shows a comparison of the counting efficiencies between the original computational phantoms and the modified (i.e., water-filled) homogeneous computational phantoms used to investigate the influence of the tissue distribution of the internal organs on the whole-body counting measurement. No significant differences (<5%) are observed between the original and modified phantoms for both WBCs. These results show that the existence of the internal organs indeed does not significantly affect the counting efficiencies. Thus, this study focused on the size dependency on the whole-body counting efficiency of the main radionuclides in radiation emergencies.

The counting efficiencies of the photo-peaks for ^{57}Co (122.1 keV), ^{134}Cs (603.7 keV), ^{137}Cs (661.6 keV), and ^{60}Co (1173.2 keV) were obtained from the 19 computational phantoms. Based on the weight and height of the computational phantoms, the BBI was calculated as $(W/H)^{1/2}$. Figs. 5 and 6 show the variations in the counting efficiencies as a function of the BBI for the computational phantoms used for the stand-up and bed type WBCs, respectively. The results show that the counting efficiencies decrease with an increase in the BBI. The variations of the counting efficiencies for each photo-peak against the BBI are similar for both systems. This is due to the gamma ray attenuation within the phantom, which leads to differences in the counting efficiency depending on the size of the subject [2]. Gamma-rays were more attenuated inside the phantoms for higher BBIs.

Linear regression was used to derive the equations for estimating the counting efficiencies, considering the individual's body size. The agreement between the fitted curve value and data points was evaluated using the coefficient of determination (R^2), which indicated that the equation matched well with the distribution of data in the whole-body measurement systems ($R^2 > 0.5$) The R^2 values for ^{60}Co (0.8514 and 0.5378 in the stand-up and bed type WBCs, respectively) are lower than those for the other radionuclides. Moreover, the regression slopes for the 1173.2 keV curve are gentle compared to those for the 122.1 keV curve. This is because the attenuation is more significant for low-energy gamma rays than for high-energy gamma rays. Hence, the counting efficiencies for the high-energy gamma-rays are less dependent on the body size than those for the low-energy gamma rays. When comparing the R^2 values of the stand-up and bed type WBCs, the agreement of the fitted curve for the stand-up type WBC is better than that for the bed type WBC. These results suggest that the measurement geometry can influence the counting efficiencies with respect to the body size of the individuals. As explained previously, the counting efficiencies of the bed type WBC are less influenced by the subject size than those of the stand-up type WBC.

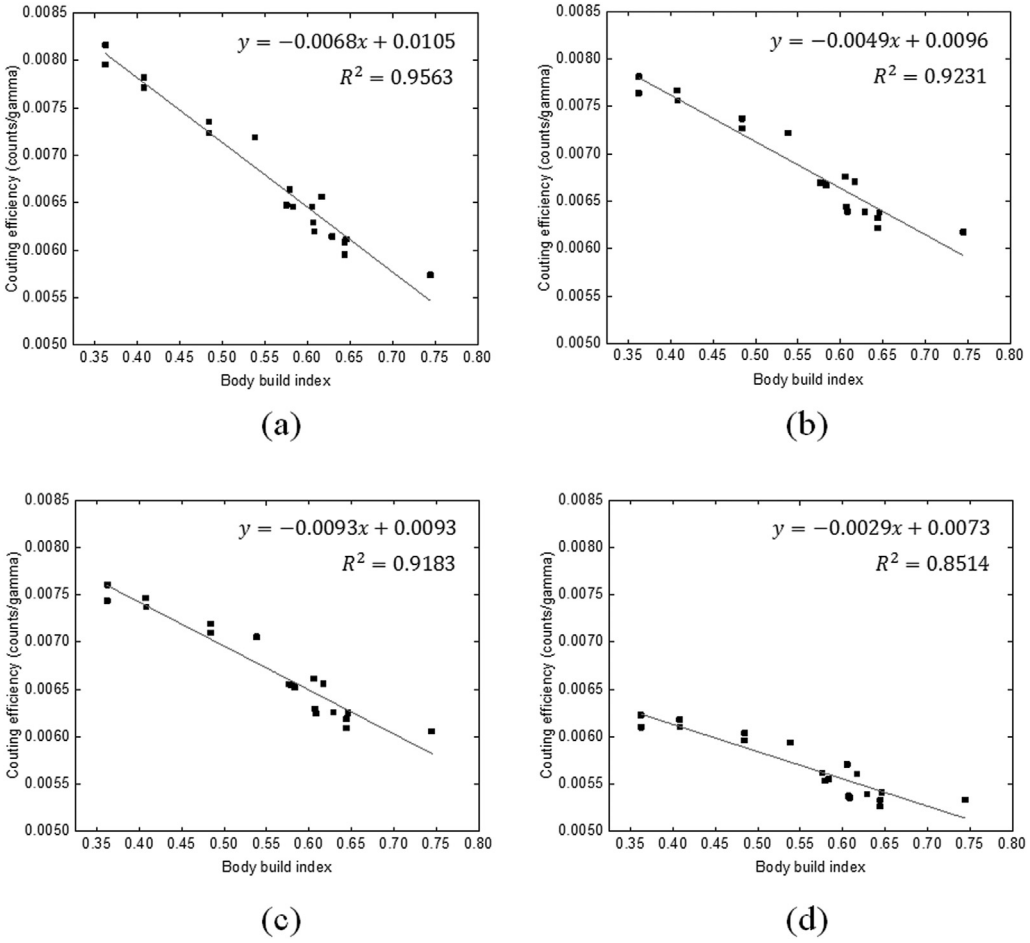

Fig. 5. Variation of the counting efficiencies for the stand-up type WBC as a function of the BBI: (a) 122.1 keV for ^{57}Co, (b) 603.7 keV for ^{134}Cs, (c) 661.6 keV for ^{137}Cs, and (d) 1173.2 keV for ^{60}Co.

The counting efficiencies in *in vivo* measurements can be influenced by the geometrical differences between the physical calibration phantom and the measured individuals. It is difficult to reproduce the calibration geometry in whole-body measurements, because individual physical characteristics differ from those of the physical calibration phantoms [12]. Furthermore, the subjects in the whole-body counting measurement vary in age, gender, and physical characteristics. Therefore, the individual physical characteristics, especially body size, should be considered to reduce the uncertainty associated with whole-body measurement results. An age-dependent efficiency calibration of WBCs is necessary to guarantee the accuracy of results when quantifying the body burden of gamma emitter incorporated contaminants in a case of public exposure e.g., after a nuclear emergency. Other approaches for virtually calibrating whole-body counting measurement systems have been investigated using simplified mathematical phantoms with different sizes by employing Monte Carlo simulation [10,14,19]. These phantoms, however, have limited information on human anatomy, which result in inaccurate measurements. In the present study, therefore, computational phantoms representing a realistic human model were used to reduce the size dependency of the counting efficiencies, thereby improving the accuracy of whole-body measurements. Based on the fitted equations presented in Figs. 5 and 6, the individualized counting efficiency in terms of the body size, can be calculated using the BBI for both systems.

4. Conclusions

In the present study, a virtual calibration was performed to calculate the whole-body counting efficiencies using Monte Carlo simulation with 19 computational phantoms of different sizes for commercial stand-up and bed type WBC systems. Monte Carlo simulations with computation al phantoms that serve as realistic human models could determine the effect of body size on the counting efficiencies. The equations for estimating individualized counting efficiencies were derived based on the relationship between the counting efficiencies and body sizes of individuals for different radionuclides of significant concern in radiation emergencies. The results demonstrate that the counting efficiency is significantly affected by the geometrical discrepancy between the physical calibration phantom and individual body characteristics of measured individuals. Our results can help determine individualized counting efficiencies in whole-body counting measurements. Biokinetic models were not considered in the present study, and the counting efficiency in the context of biokinetic models should be investigated in the future to realize the accurate measurement of internal contamination.

Declaration of competing interest

The authors declare that they have no known competing

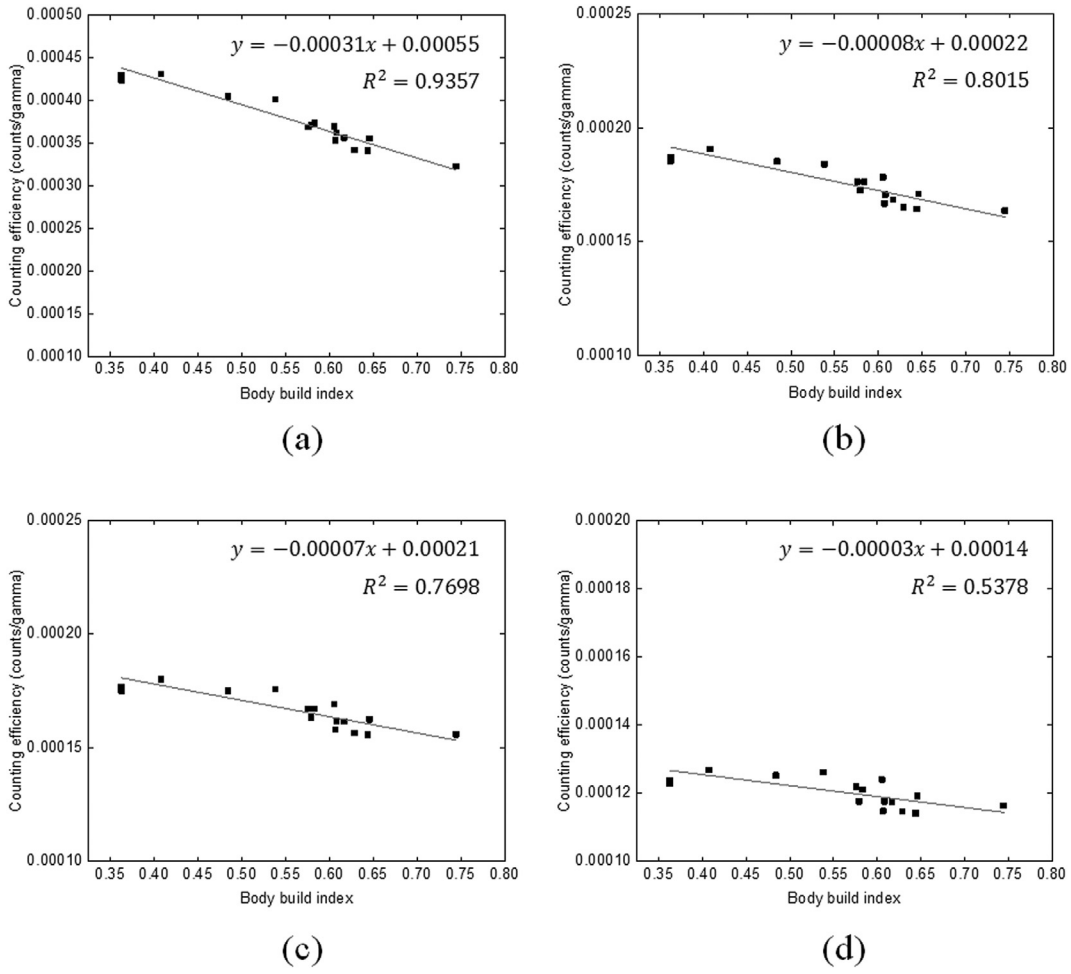

Fig. 6. Variation of the counting efficiencies for the bed type WBC as a function of the BBI: (a) 122.1 keV for ^{57}Co, (b) 603.7 keV for ^{134}Cs, (c) 661.6 keV for ^{137}Cs, and (d) 1173.2 keV for ^{60}Co.

financial interests or personal relationships that could have appeared to influence the work reported in this paper.

Acknowledgments

This study was supported by a grant of the Korea Institute of Radiological and Medical Sciences (KIRAMS), funded by Ministry of Science and ICT(MSIT), Republic of Korea. (No.50535–2021) The authors would like to express their gratitude to Choonsik Lee at the National Cancer Institute, X. George Xu at the Rensselaer Polytechnic Institute, Richard Kramer at the Federal University of Pernambuco, and Kaoru Sato at the Japan Atomic Energy Agency for providing valuable data on computational phantoms.

References

[1] K. Tani, Y. Igarashi, E. Kim, T. Iimoto, O. Kurihara, Monte-Carlo simulations with mathematical phantoms to investigate the effectiveness of a whole-body counter for thyroid measurement, Radiat. Meas. 135 (2020), https://doi.org/10.1016/j.radmeas.2020.106335. http://www.ncbi.nlm.nih.gov/pubmed/106335.

[2] O. Kurihara, C. Li, M.A. Lopez, E. Kim, K. Tani, T. Nakano, C. Takada, T. Momose, M. Akashi, Experiences of population monitoring using whole-body counters in response to the Fukushima nuclear accident, Health Phys. 115 (2) (2018) 259–274, https://doi.org/10.1097/HP.0000000000000862. https://www.ncbi.nlm.nih.gov/pubmed/29957688.

[3] E. Kim, O. Kurihara, N. Kunishima, T. Nakano, K. Tani, M. Hachiya, T. Momose, T. Ishikawa, S. Tokonami, M. Hosoda, M. Akashi, Early intake of radiocesium by residents living near the TEPCO Fukushima Dai-ichi nuclear power plant after the accident. Part 1: internal doses based on whole-body measurements by NIRS, Health Phys. 111 (5) (2016) 451–464, https://doi.org/10.1097/HP.0000000000000563. https://www.ncbi.nlm.nih.gov/pubmed/27682904.

[4] N. Matsuda, A. Kumagai, A. Ohtsuru, N. Morita, M. Miura, M. Yoshida, T. Kudo, N. Takamura, S. Yamashita, Assessment of internal exposure doses in Fukushima by a whole body counter within one month after the nuclear power plant accident, Radiat. Res. 179 (6) (2013) 663–668, https://doi.org/10.1667/RR3232.1. https://www.ncbi.nlm.nih.gov/pubmed/23642080.

[5] Health Physics Society, American National Standard: specifications for the bottle manikin absorption phantom, ANSI/HPS N13 (1999) 35.

[6] R. Toohey, E. Palmer, L. Anderson, C. Berger, N. Cohen, G. Eisele, B. Wachholz, W. Burr Jr., Current status of whole-body counting as a means to detect and quantify previous exposure to radioactive materials, Whole-body Counting Working Group, Health Phys. 60 (Suppl. 1) (1991) 7–42.

[7] D.R. White, The design and manufacture of anthropomorphic phantoms, Radiat. Protect. Dosim. 49 (1–3) (1993) 359–369, https://doi.org/10.1093/rpd/49.1-3.359.

[8] B. Zhang, M. Mille, X.G. Xu, An analysis of dependency of counting efficiency on worker anatomy for in vivo measurements: whole-body counting, Phys. Med. Biol. 53 (13) (2008) 3463–3475, https://doi.org/10.1088/0031-9155/53/13/004. https://www.ncbi.nlm.nih.gov/pubmed/18547914.

[9] J. Bento, S. Barros, P. Teles, P. Vaz, M. Zankl, Efficiency correction factors of an ACCUSCAN whole-body counter due to the biodistribution of ^{134}Cs, ^{137}Cs and ^{60}Co, Radiat. Protect. Dosim. 155 (1) (2013) 16–24, https://doi.org/10.1093/rpd/ncs308. https://www.ncbi.nlm.nih.gov/pubmed/23188813.

[10] R.J. Shypailo, K.J. Ellis, Whole body counter calibration using Monte Carlo modelling with an array of phantom sizes based on national anthropometric reference data, Phys. Med. Biol. 56 (10) (2011) 2979–2997, https://doi.org/10.1088/0031-9155/56/10/006. https://www.ncbi.nlm.nih.gov/pubmed/21490381.

[11] E. Carinou, V. Koukouliou, M. Budayova, C. Potiriadis, V. Kamenopoulou, The calculation of a size correction factor for a whole-body counter, Nucl. Instrum. Methods Phys. Res. 580 (1) (2007) 197–200, https://doi.org/10.1016/

j.nima.2007.05.083.
[12] D. Krstic, O. Cuknic, D. Nikezic, Application of MCNP5 software for efficiency calculation of a whole body counter, Health Phys. 102 (6) (2012) 657–663, https://doi.org/10.1097/HP.0b013e318244152b.
[13] M. Park, J. Yoo, W.H. Ha, S. Park, Y.W. Jin, Measurement and simulation of the counting efficiency of a whole-body counter using a BOMAB phantom inserted with rod sources containing mixed radionuclides, Health Phys. 114 (3) (2018) 282–287, https://doi.org/10.1097/HP.0000000000000752. https://www.ncbi.nlm.nih.gov/pubmed/29360706.
[14] G.H. Kramer, K. Capello, The STANDFAST whole body counter: efficiency as a function of BOMAB phantom size and energy modeled by MCNP5, Health Phys. 92 (3) (2007) 290–296, https://doi.org/10.1097/01.HP.0000246233.61967.3a. https://www.ncbi.nlm.nih.gov/pubmed/17293701.
[15] Y. Chen, R. Qiu, C. Li, Z. Wu, J. Li, Construction of Chinese adult male phantom library and its application in the virtual calibration of in vivo measurement, Phys. Med. Biol. 61 (5) (2016) 2124–2144, https://doi.org/10.1088/0031-9155/61/5/2124. https://www.ncbi.nlm.nih.gov/pubmed/26894453.
[16] S. Kinase, S. Takagi, H. Noguchi, K. Saito, Application of voxel phantoms and Monte Carlo method to whole-body counter calibration, Radiat. Protect. Dosim. 125 (1–4) (2007) 189–193, https://doi.org/10.1093/rpd/ncm197.
[17] M. Takahashi, S. Kinase, R. Kramer, Evaluation of counting efficiencies of a whole-body counter using Monte Carlo simulation with voxel phantoms, Radiat. Protect. Dosim. 144 (1–4) (2011) 407–410, https://doi.org/10.1093/rpd/ncm417.
[18] M. Park, T.E. Kwon, W.H. Ha, C.H. Kim, S. Park, Y.W. Jin, Counting efficiencies determined by Monte Carlo methods for in vivo measurement of 131I activity in thyroid, Health Phys. 117 (4) (2019) 388–395, https://doi.org/10.1097/HP.0000000000001070. https://www.ncbi.nlm.nih.gov/pubmed/30913058.
[19] G.H. Kramer, L.C. Burns, S. Guerriere, Monte Carlo simulation of a scanning detector whole body counter and the effect of BOMAB phantom size on the calibration, Health Phys. 83 (4) (2002) 526–533, https://doi.org/10.1097/00004032-200210000-00011. https://www.ncbi.nlm.nih.gov/pubmed/12240728.
[20] J. Bento, S. Barros, P. Teles, M. Neves, I. Gonçalves, J. Corisco, P. Vaz, Monte Carlo simulation of the movement and detection efficiency of a whole-body counting system using a BOMAB phantom, Radiat. Protect. Dosim. 148 (4) (2012) 403–413, https://doi.org/10.1093/rpd/ncr201. https://www.ncbi.nlm.nih.gov/pubmed/21525044.
[21] C.J. Werner, MCNP User's Manual Code Version 6.2, Los Alamos National Laboratory, 2017. LA-UR-17-29981.
[22] ICRP 110, Adult Reference Computational Phantoms vol. 110, Pergamon Press Publication, Oxford, 2009.
[23] C. Lee, D. Lodwick, J. Hurtado, D. Pafundi, J.L. Williams, W.E. Bolch, The UF family of reference hybrid phantoms for computational radiation dosimetry, Phys. Med. Biol. 55 (2) (2010) 339–363, https://doi.org/10.1088/0031-9155/55/2/002. https://www.ncbi.nlm.nih.gov/pubmed/20019401.
[24] C.H. Kim, S.H. Choi, J.H. Jeong, C. Lee, M.S. Chung, HDRK-Man: a whole-body voxel model based on high-resolution color slice images of a Korean adult male cadaver, Phys. Med. Biol. 53 (15) (2008) 4093–4106, https://doi.org/10.1088/0031-9155/53/15/006. https://www.ncbi.nlm.nih.gov/pubmed/18612173.
[25] Y.S. Yeom, J.H. Jeong, C.H. Kim, M.C. Han, B.K. Ham, K.W. Cho, S.B. Hwang, HDRK-Woman: whole-body voxel model based on high-resolution color slice images of Korean adult female cadaver, Phys. Med. Biol. 59 (14) (2014) 3969–3984, https://doi.org/10.1088/0031-9155/59/14/3969. https://www.ncbi.nlm.nih.gov/pubmed/24971755.
[26] X.G. Xu, T.C. Chao, A. Bozkurt, VIP-Man: an image-based whole-body adult male model constructed from color photographs of the visible human project for multi-particle Monte Carlo calculations, Health Phys. 78 (5) (2000) 476–486, https://doi.org/10.1097/00004032-200005000-00003. https://www.ncbi.nlm.nih.gov/pubmed/10772019.
[27] K. Sato, H. Noguchi, Y. Emoto, S. Koga, K. Saito, Japanese adult male voxel phantom constructed on the basis of CT images, Radiat. Protect. Dosim. 123 (3) (2007) 337–344, https://doi.org/10.1093/rpd/ncl101. https://www.ncbi.nlm.nih.gov/pubmed/16905760.
[28] K. Sato, H. Noguchi, Y. Emoto, S. Koga, K. Saito, Development of a Japanese adult female voxel phantom, J. Nucl. Sci. Technol. 46 (9) (2009) 907–913, https://doi.org/10.1080/18811248.2009.9711599.
[29] F. Cassola, V.J. Lima, R. Kramer, H.J. Khoury, FASH and MASH: female and male adult human phantoms based on polygon mesh surfaces: I. Development of the anatomy, Phys. Med. Biol. 55 (1) (2010) 133–162, https://doi.org/10.1088/0031-9155/55/1/009. https://www.ncbi.nlm.nih.gov/pubmed/20009183.
[30] T. Smith, R. Hesp, J. Mackenzie, Total body potassium calibrations for normal and obese subjects in two types of whole body counter, Phys. Med. Biol. 24 (1) (1979) 171–175, https://doi.org/10.1088/0031-9155/24/1/016. https://www.ncbi.nlm.nih.gov/pubmed/107535.
[31] A. Lahham, M. Fulop, M. Vladar, P. Ragan, Body potassium content and radiation dose from 40K to the Slovak population, Health Phys. 74 (3) (1998) 346–349, https://doi.org/10.1097/00004032-199803000-00007.